Qatar Univ. Sci. J. (2000), 20 : 181 - 195

GEOCHEMISTRY AND PETROGENESIS OF A LATE PROTEROZOIC VOLCANIC SEQUENCE IN THE MAGAL GEBRIEL AREA, SOUTH EASTERN DESERT, EGYPT

By

S.M. El-Shazly[1] and H.A. Hegazy[2]

[1] Department of Geology, Alexandria University, Alexandria, Egypt

[2] Department of Geology, Assiut University, Assiut, Egypt

جيوكيميائية وأصل التتابع البركاني ذو العصر البروتيروزوي المتأخر بمنطقة مجال جبريل جنوب الصحراء الشرقية - مصر

سمير محمود الشاذلي — قسم الجيولوجيا - جامعة الأسكندرية - مصر

حسين عزيز حجازي — قسم الجيولوجيا - جامعة أسيوط - مصر

تُكَوِّن صخورالميتابازلت والميتااندیزیت الجزء الأكبر من الصخور السطحية بمنطقة مجال جبريل كما توجد كمية بسيطة من صخور الميتاداسيت، توجد كذلك بمنطقة الدراسة كمية محدودة من صخر الربوليت الغير متحول، تظهر صخورالبركانيات المتحولة مدى كبير لرقم الماغنسيوم (٠,٣٨ - ٠,٧١) كما أنها تتميز بارتفاع قيم العناصر ذات أنصاف الأقطار الكبيرة وكذلك قيم العناصر الأرضية النادرة الخفيفة، بينما تتميز صخور الربوليت بالقيم العالية لأكسيد السليكا (٧٢ - ٧٦,٦٪) وعنصر الزركونيوم وكذلك العناصر ذات أنصاف الأقطار الكبيرة والعناصر الأرضية النادرة الخفيفة كما تتميز بالقيم المنخفضة لأكسيد التيتانيوم وعنصري السكانديوم والفانديوم، وقد وجد أن عملية التفارق تلعب دوراً هاماً في نشأة الصخور المتوسطة من الصخور القاعدية عن طريق خروج البروكسين، والبلاجيوكلازا والمعادن المعتمة، صخور البركانيات المتحولة بمنطقة مجال جبريل لها وضع تكتوني مشابه للجزر القوسية بينما تتميز صخور الريوليت بوضع تكتوني يشبه مناطق داخل الألواح.

مخطط العناصر الأرضية النادرة الثقيلة لا يظهر أي تفارق بالنسبة لصخور البركانيات المتحولة مما يشير إلى أن هذه الصخور قد نشأت من منطقة وشاح خالية من الجارنت، ويمكن أن يكون الصهير الأصلي قد نشأ نتيجة انصهار جزئي بسيط (٥-٨٪) لصخور وشاح تعرضت لعملية نضوب سابقة مماأدى إلى تكوين الصخور الأولية ذات التركيب البازلتي، أما عمليات التفارق اللاحقة فقد كونت باقي الصخور الموجودة في منطقة الدراسة، تشير النماذج المحسوبة أن القيم المطلقة للعناصر القابلة للحركة في منطقة الأندساس أقل من مثيلاتها المحسوبة في الجزر القوسية بمناطق أخرى مثل غرب الباسيفك والمكسيك ولكن بنفس درجة التتابع في الزيادة: باريوم > روبيديوم > بوتاسيوم > لانثانيوم > استرنشيوم > سيريوم.

مخططات العناصر الأرضية النادرة لصخور الريوليت توازي مخططات الصخور البركانية المتحولة كما تتميز أيضاً بعدم وجود تفارق في مخططات العناصر الأرضية النادرة الثقيلة وهذه الخصائص تدل على أن المجما الأم لكل من الريوليت والصخور المتحولة متشابهة، ولكن المجما الأم لصخور الربوليت لابد وأن تكون قد تعرضت لعملية تفارق شديدة وخروج لكميات كبيرة من البلاجيو كلازويستدل على ذلك من القيم الشاذة السالبة العالية لعنصر البوربيوم وكذلك من القيم المنخفضة لعنصر الاسترنشيوم.

Key Words : Magal Gebriel, Metavolcanics, Rhyolite, Rhyolite porphyry.

ABSTRACT

Metabasalts and meta-andesites together with small amounts of metadacite constitute the Magal Gebriel volanic suite. Restricted amounts of unmetamorphosed rhyolitic rocks are also present. The metavolcanics show a wide range of Mg numbers (0.38 – 0.71), and are enriched in LILE and LREE. The rhyolitic rocks are very rich in SiO_2 (72.0-76.6 wt.%), low in TiO_2, Sc, V and high in LILE and LREE. The geochemical trends defined by the basaltic to dacitic volcanic rocks suggest fractional crystallization from a basaltic liquid by removal of pyroxene, plagioclase and opaque minerals.

The Magal Gebriel metavolcanics (MGM) posses the geochemical characteristics of an island arc tectonic setting while those of the rhyolitic rocks posses that of within-plate tectonic setting. The nearly flat HREE patterns of the studied metavolcanic rocks $\{(Gd/Yb)_N = 1.2\text{-}1.5\}$ suggest that they originated from a garnet-free peridotite source. The parent magma may represent low-degree (5 - 8%) partial melts of a depleted mantle. Fractional crystallization of the primitive magma yielded the different volcanic rocks of Magal Gebriel volcanic suit. The enrichment of the subarc mantle in the subduction-derived component in Magal Gebriel area was modelled. The calculated concentrations of some mobile elements are generally lower than those estimated for other island arcs in western Pacific and Mexico but with a similar order of enrichment: Ba > Rb > K > La > Sr > Ce.

The rhyolitic rocks have REE patterns that are nearly parallel to those of the metavolcanic rocks suggesting similar parental magmas. However, the rhyolitic mother magma must have subjected to severe differentiation and extraction of large amount of plagioclase as indicated by the strong negative Eu anomalies and low Sr contents.

INTRODUCTION

Volcanic and volcaniclastic rocks cover vast areas in the Egyptian Eastern Desert and constitute important rock units, viz. the metavolcanics and Dokhan volcanics, within the Precambrian Shield. The metavolcanics are widely distributed in the central and southern parts of the Eastern Desert forming extensive outcrops, which may attain a thickness of several kilometers. They occupy about 12% of the total basement in the Eastern Desert of Egypt (Stern, 1). The metavolcanic rocks in the Central Eastern Desert are subdivided by Stern [2] into old metavolcanics (OMV) and young metavolcanics (YMV). The old metavolcanics pertain to the ophiolites and are composed predominantly of pillowed metabasalts. They are commonly spilitized and slightly metamorphosed, usually in the lower greenschist facies. In contrast, the young metavolcanics are represented mainly by andesitic flows, but mafic and more felsic volcanics together with volcaniclastic breccias and tuffs are also common. Stern [2] mentioned that the YMV were formed in an island arc and were subjected to regional metamorphism at least in the greenschist facies and rarely may reach the amphibolite facies. The Dokhan volcanics are of limited distribution and cover about 2.5% of the total basement rocks in the Eastern Desert of Egypt (Stern, 1). They are mostly located north of latitude 26(N. These rocks are unmetamorphosed and include acidic, intermediate volcanics and equivalent pyroclastics; welded tuffs and ignimbrites are also common (El-Gaby et al., 3). Rb-Sr whole rock ages of the Dokhan volcanics range between 639 and 581 Ma (Dixon, 4; Stern and Hedge, 5). El-Gaby et al. [6] believe that the Dokhan volcanics represent the surface manifestation of the synlate-tectonic, calc-alkaline granites.

In this paper we discuss the petrogenesis and tectonic evolution of a suite of metavolcanic rocks pertaining to the younger metavolcanics and ranging in composition from basalt to dacite, with help of petrographic and geochemical data. The petrogenesis of younger rhyolitic rocks with an age slightly higher than that of the Dokhan volcanics and crop out in the southeastern corner of the study area is also discussed.

GEOLOGICAL SETTING

Magal Gebriel area lies at the southern part of Eastern Desert Egypt, about 170km Southeast of Aswan city (Fig. 1). The area is covered mainly by igneous and metamorphic rocks belonging to the Precambrian Basement Complex. The rocks in this area comprise a low grade metamorphosed volcano-sedimentary succession intruded by granitoid rocks (old and young granitoids). The metasediments are the oldest rock units in Megal Gebriel district and crop out mainly as isolated masses in the southern and western parts of the study area. They form low to moderate exposures of greyish and blackish green colours and are invaded by different rock types including the metavolcanics and granites. The metasediments comprise intercalated biotie schist, chlorite schist, quartzofeldspathic schist and tremolite-bearing marble and have a general

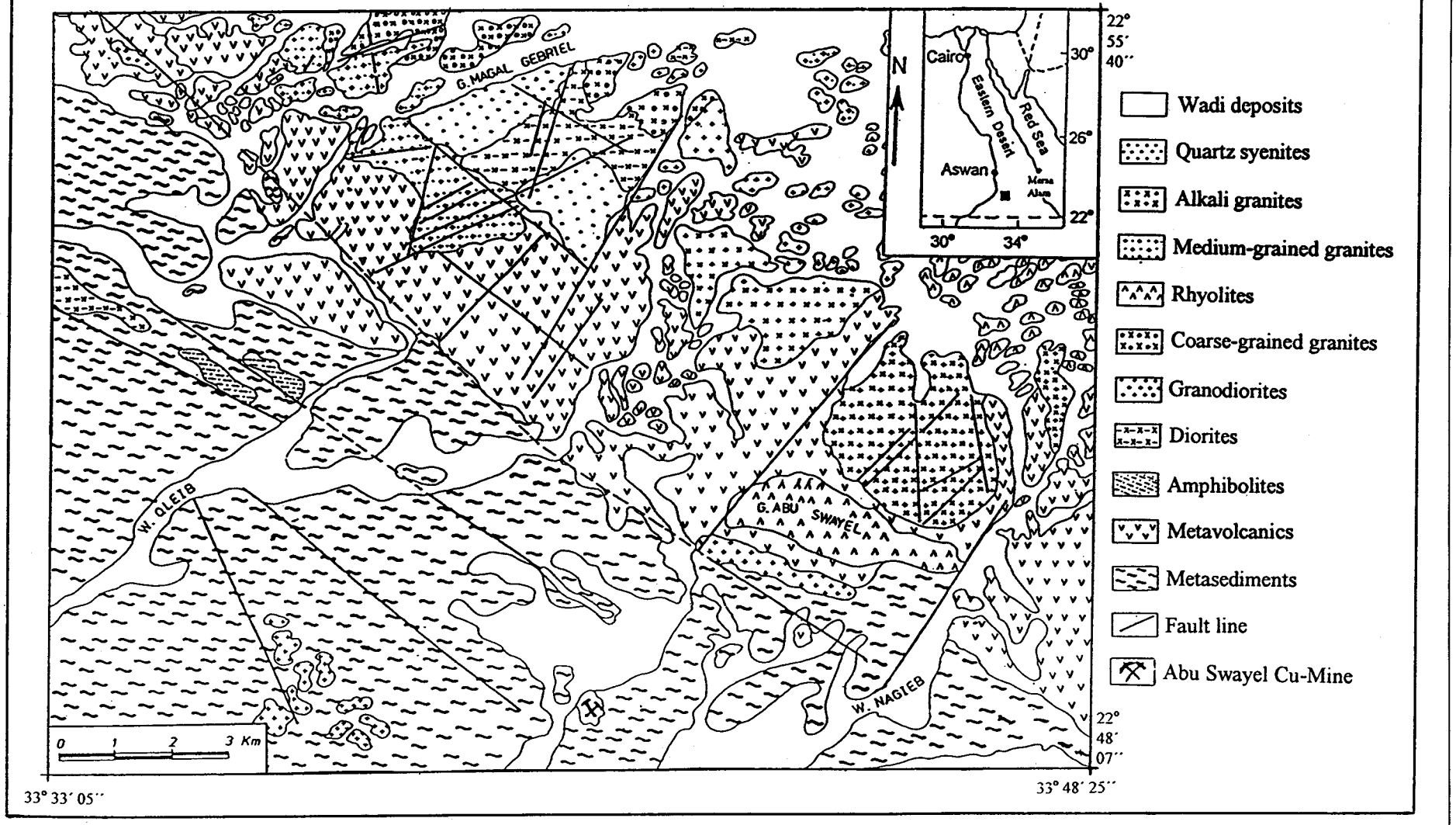

Fig.1: Geological map of the Magal Gebriel area. After Farag [7]

direction of foliation trending NW-SE. The metavolcanics crop out in the central and eastern parts of the study area forming low to moderate relief ridges. They are intruded by granitic rocks commonly along sharp and irregular intrusive contacts. Metabasalt and meta-andesite are the most common rock types of the Megal Gebriel volcanic rocks that pertain to the younger metavolcanics, however, few metadacites are also present.

Different granitic rocks are observed in the study area including coarse-grained, pale pink granite, medium-grained granite and alkali feldspar granite. The coarse-grained granite is restricted to the northern part of the study area and may be correlated with the synorogenic subduction-related, I-type older granites (G1) according tot he classification of Hussein et al. [8]. They are invaded by the medium-grained granite, which corresponds to the younger graintes (G2) of Hussein et al. [8]. The medium-grained granites form moderate to high lying outcrops in the north central parts of the study area. They have sharp intrusive contacts against the metavolcanics and coarse-grained granites. The alkali feldspar granitic rocks are mainly located in the eastern part of the study area. They are intruded in the metavolcanics along sharp intrusive contacts. The are arranged in NNW-SSE direction, which is nearly concordant with the major foliation of the metasediments. The alkali feldspar granitic rocks may be correlated with the crustal intraplate granites (G3) of Hussein et al. [8].

Restricted amounts of rhyolite and rhyolite porphyry form another member of Magal Gebriel volcanic suite. These rhyolite rocks (654-665 Ma, El-Shazly et al., 9) form the main outcrop of Gebel Abu Swayel that intrude the metavolcanics and metasediments as large extrusive in the southeastern part of the study area. The given age of the rhyolites is somewhat higher than that of the unmetamorphosed Dokhan volcanics.

The Megal Gebriel area is dissected by a series of faults; the most common trends are NE-SW, NW-SE, ENE-WSW, NNE-SSW and E-W.

PETROGRAPHY

The metabasalts range in texture from aphyric to porphyritic with small phenocrysts of plagioclase and clinophyroxene in a fine-grained matrix. Ophitic texture is also common and well preserved. The clinopyroxenes are represented by augite that is partially or completely altered to actinolite, tremolite and chlorite. The plagoiclase crystals (An_{48-60}) are highly sericitized. The metandesites are genrally porphyritic and contain phenocrysts of plagioclase (An_{42-52}) and amphibole enclosed in a fine-grained groundmass of plagioclase and amphibole with accessory quartz. The plagioclase feldspar phenocrysts as well as those of the groundmass are highly sericitized, while the amphibole is altered to chlorite and epidote. Fe-Ti oxides are common in the groundmass of the metabasalt and metandesite forming up to 8 vol.% in some rocks. The metabasalts and meta-andesites are the most predominant rock types in Megal Gebriel area . There is a gradation between them forming metabasaltic andesites. The metadacites cover small outcrops of the study area. They are composed mainly of small phenocrysts of plagioclase and quartz in a very fine-grained groundmass of the same constituents. This rock type is very poor in ferromagnesian minerals that are completely altered when present. The metavolcanic rocks of the study area have a mineral assemblage indicating low to moderate degree of regional metamorphism corresponding to the greenschist and low amphibolite facies.

The rhyolites are fine-to medium-grained unmetamorphosed rocks with a characteristic pale pink colour. They are composed mainly of K-feldspar, quartz and sodic plagioclase as well as small flakes of muscovite and biotite. The feldspars are commonly fresh but few crystals are slightly altered to sericite. The rock is very poor in ferromagnesian minerals. Fe-Ti oxides and zircon are the main accessories. The spherulitic intergrowth between K-feldspar and quartz is characteristic. Some porphyritic varieties are occasionally observed particularly at the margin of the mass, they contain phenocrysts mainly of K-feldspar and quartz. The matrix includes microcrystalline plagioclase, K-feldspar, Fe-Ti oxides, muscovite and biotite.

GEOCHEMISTRY

Major and trace element analyses of 28 samples were performed by the X-ray fluorescence (XRF) method using a fully automated Philips 24000 Spectrometer. Rare earth elements (REE) were analyzed by ICP-MS, after ion-exchange separation. The analyses were carried out at the Mineralogical Institute of Cologne University, Germany. Accuracies, as determined by replicate analyses, are stimated at better than 1% for SiO_2, Al_2O_3, Fe_2O_3, and CaO and from 1-3% for the other oxides. On the other hand, trace element errors are generally less than 10%. The analystical results are given in

Table1. The composition range of Magal Gebriel metavolcanics (metabasalt, metabasaltic andesite, metandesite and metadacite) is demonstrated using the SiO_2 versus Zr/TiO_2 and Zr/TiO_2 versus Nb/Y diagrams (Winchester and Floyd, 10: figures are not shown). The metavolcanics show a wide range of Mg number (0.38 – 0.71) and are quartz, diopside and hypersthene normative. They are enriched in the large ion lithophile elements (LILE) and light rare earth elements (LREE). The rhyolitic rocks are rich in SiO_2 (72 – 76.6 wt.%) and are characterized by low TiO_2, Sc, V and high LILE and LREE.

A major problem in the study of metavolcanic sequences is the possible effects of metamorphism, which may change the original chemical composition. The effects of alkaline metasomatism on the mafic magmatic rocks can be illustrated using the (K_2O+Na_2O) vs. $100*K_2O/(K_20+Na_2O)$ diagram (Hughes, 11). It is clear from this diagram (Fig. 2) that most of the studied samples are located in the filed of "igneous spectrum", few samples seem to have signs of crustal contaimnation with potassium enrichment trend. On the other hand, two andestic samples show a slight trend toward Na_2O enrichment that might suggest the effect of marine water on these rocks. All the samples plot in the field of unaltered rocks on the ternary diagram CaO/Al_2O_3 – $MgO/10$ – $SiO_2/10$ (Fig. 3) after Davis et al. [12]. However, the petrogenesis and tectonic setting of the studied rocks are interpreted mainly using the immobile trace elements and REE. The samples that were chosen for geochemical analyses werr examined petrographically for evidences of significant alteration, metasomatism, mineral disequalibrium, and unusual mineral assemblages. It is worthy to mention that sample no. "1" possesses unusual enrichment in TiO_2, Y and Nb, it has also high total iron content resulting in a low Mg # (Table 1). This sample is not representative of the suite and is excluded from any petrogenetic interpretation.

The Megal Gebriel metavolcanics (MGM) are sub-alkaline in nature in terms of $(Na_2O + K_2O)$ versus SiO_2 classification (Irvine and baragar, 13). They show a transitional tholeiitic/calc-alkaline affinity on the AFM diagram (Fig. 4; Irvine and Baragar, 13). The MGM fall in the fields of volcanic arc

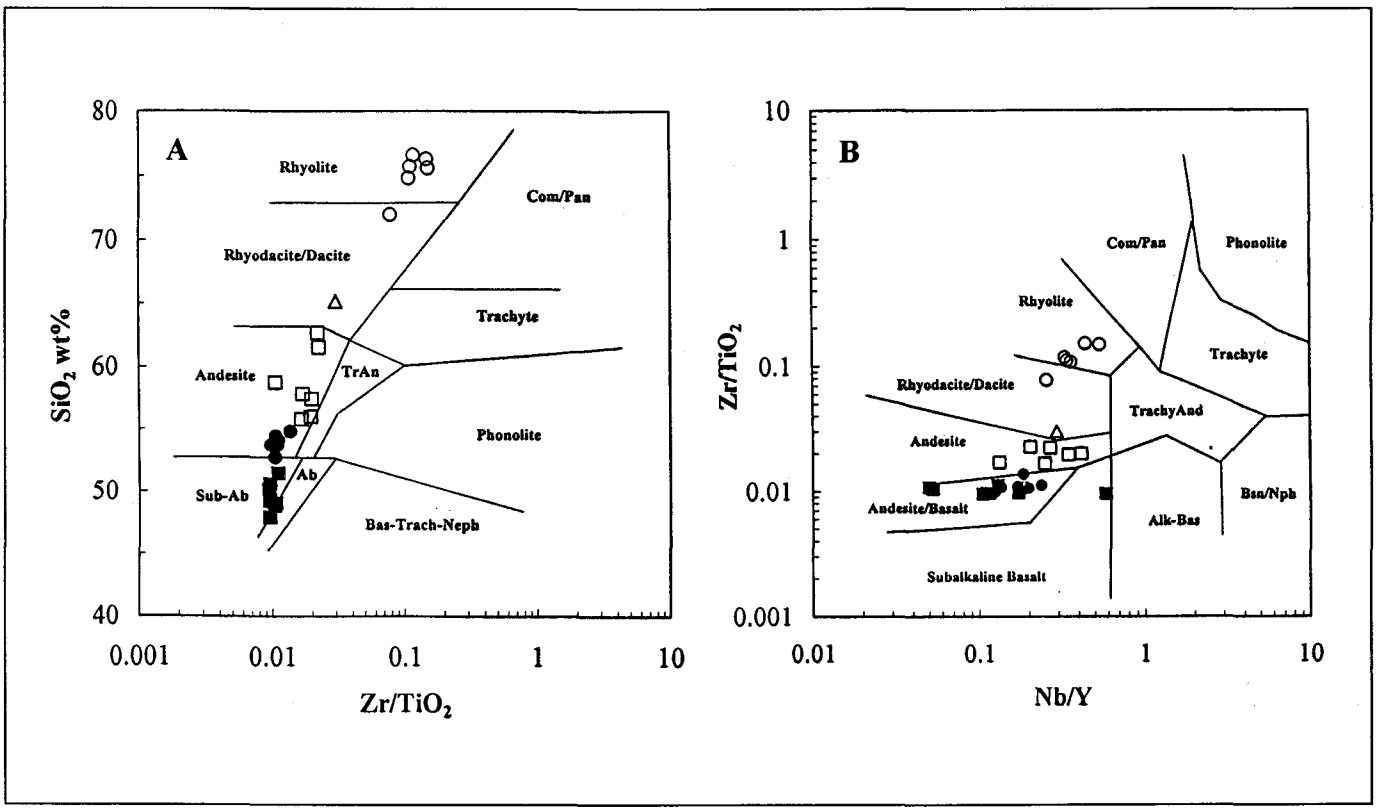

Fig. 2A & B : SiO_2 vs Zr/TiO_2 and Zr/TiO_2 vs Nb/Y discrimination diagrams (after Winchester and Floyd, 10) for the different rock types of Magal Gebriel area. ■ : Metabasalt, ● : Metabasaltic andesite, ❑ : Metandesite, ❑ : Meta-andesite, ❑ Metadacite, ❑ : Rhyolite

basalt (Vab) and island arc tholeiite (IAT) on the Nb-Zr-Y (Meschede, 14) and the TiO_2 – MnO – p_2O_5 (Mullen, 15) discrimination diagrams (Figs. 5 and 6). In contrast, the rhyolitic rocks fall mainly within the domain of within-plate granite on the Nb-Y and Rb–Y+Nb (Pearce et al., 16) variation diagrams (Fig.7). All the studied metavolcanics show prominent enrichment of the LILE (K, Rb, Ba and Th) an depletion in HFSE (Zr, Y and Yb) on the MORB-normalized spider diagram (Figs. 8A & B). The enrichment of LILE relative to HFSE is considered to be one of the most critical evidences of volcanic arc magmatism. All the normalized patterns have a marked trough in Nb and most of them show negative P and Ti anomalies that support the island arc tectonic setting of the MGM. Most of the elements used in the normalized plot, except for Sr, Ba and possibly Ti, are incompatible and hence the shape of the patterns does not depend on the degree of partial melting or fractional crystallization that the rocks have experienced (Pearce, 17). These processes affect only the absolute concentrations of the incompatible elements. The patterns of both the basic and more evolved varieties of MGM are similar and show the same general features, namely enrichment in LILE and depletion in HFSE. Enrichment in LILE above normal MORB values has been attributed to the transport of these elements by hydrous fluids resulted from the subducting slab (Saunders and Tarney, 18). Sample from the MGM show REE contents that increase from metabasalt through metandesite to metadacite, while the negative Eu anomalies become progressively more pronounced from metabasalt to metadacite (Eu/Eu* = 0.70 – 0.54). The REE patterns (Fig.9) show variable LREE enrichment with $(La/Sm)_N$ ratios ranging from 2.11 to 2.76 and $(La/Yb)_N$ ratios from 3.12 to 4.25. The rhyolites display more fractionated REE patterns {$(La/Yb)_N$ = 4.7, on average} and are characterized by strong negative Eu anomalies (Eu/Eu* = 0.15, on average). The REE patterns of the metavolcanics and rhyolites have nearly flat and unfractionated HREE where the $(Gd/Yb)_N$ ratio varies between 1.2 and 1.5 for the different rock types of the metavolcanics and has an average of 1.01 for the rhyolites. The increase of $(La/Yb)_N$ ratio from 3.12 in the metabasalt to 4.25 in the metadacite suggests clinopyroxene fractionation because the removal of clinopyrozene would enrich the remaining melt in LREE more than in HREE (Arth, 19).

DISCUSSION

The most primitive rocks of the metavolcanics in Megal Gebriel area have a basaltic composition, while dacites represent the more evolved rocks. The broad geochemical trends that are defined by these rocks suggest increasing degree of differentiation. At low values of SiO_2, the relatively undifferentiated rocks have high MgO, CaO, MnO, TiO_2, Sr, V and Sc and low imcompatible trace element abundances. At high values of SiO_2, the more differentiated rocks have lower abundances of the above-mentioned elements, and higher incom-

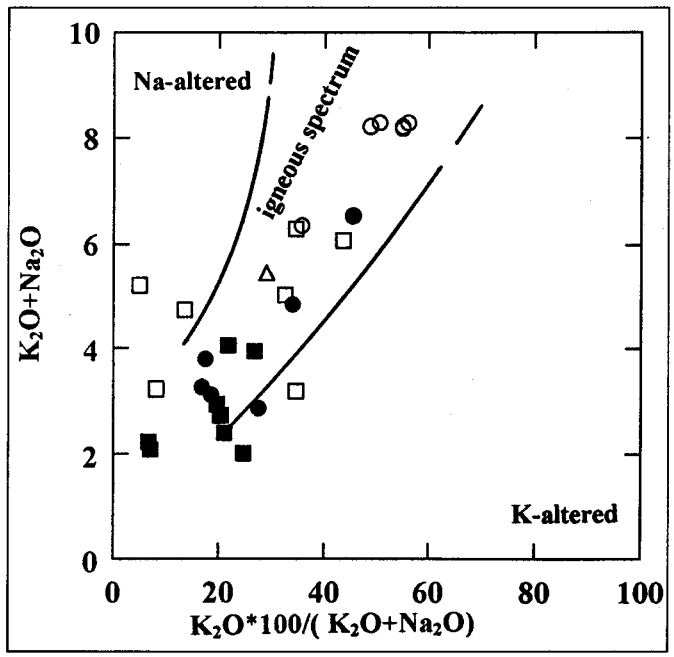

Fig. 3 : K_2O+Na_2O vs $K_2O*100/(K_2O+Na_2O)$ variation diagram, (after Hughes, 11). Symbols as in Fig. 2.

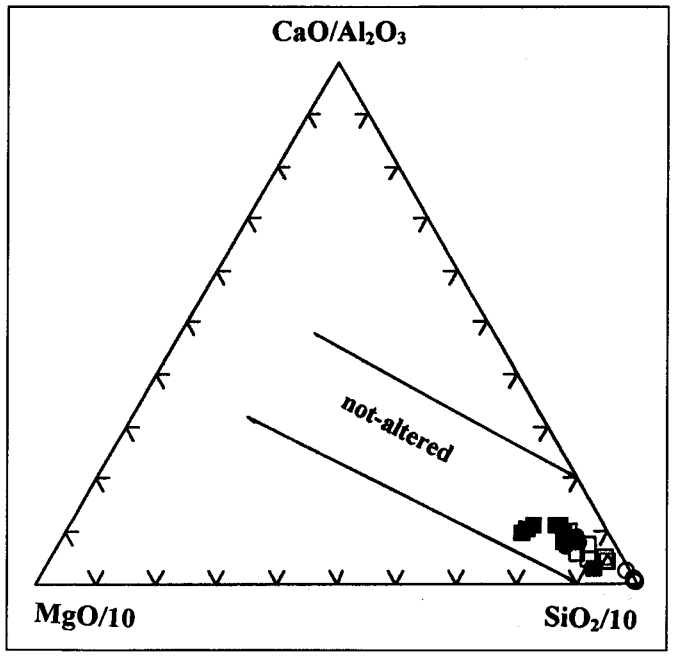

Fig. 4 : The Mgo/10-CaO/Al_2O_3-SiO_2/100 ternary plot of the Magal Gebriel volcanic rocks, (after Davis et al., 12). Symbols as in Fig. 2.

patible trace element concentrations. The increasing degree of differentiation is also reflected in the REE patterns, changing from less fractionated patters with small negative Eu anomalies in the metabasalt to more fractionated patters with more pronounced negative Eu anomalies in the metadacite. REE concentrations increase from metabasalt to metadacite accompanied by a general increase in $(La/Sm)_N$ ration. The observed variations suggest franctional crystallization of pyroxene, plagioclase and opaque minerals from a basaltic liquid.

The Magal Gebriel rocks have a composition similar to that found in modern island-arc basalt (IAB) as indicated by their elevated LILE, depleted Nb, Ti, P and HFSE. The plotting of the metavolcanics on the various discrimination diagrams confirms the island-arc tectonic setting of these rocks. The metavolcanics have an affinity transitional from tholeiitic and calc alkaline suites, which may be interpreted as representing immature/mature island-arc tectonic setting. The metavolcanic rocks of Megal Gebriel area contain some primitive varieties of basaltic composition (Samples no. 2,3,5 and 6), which have whole rock MgO (7.6-9.3 wt %), Mg # (0.63 – 0.71) and Ni (147 – 286 ppm) that are close to those expected of mantle peridotite partial melts. In contrast, most of the compositional range of MGM does not represent true mantle melts but has undergone different degrees of franctionation. The primitive varieties provide valuable probes for assessing the composition and generation of MGM parental magma.

The chemical characteristics of the most primitive rocks from MGM suggest generation from a mantle source region that is enriched in LILE and LREE relative to the HFSE. This pattern is common for arc basalts wordwide (Pearce and Peate, 20). The most primitive rocks from MGM have low concentrations of the high field strength elements Ti (4736 – 4916 ppm), Zr (77 – 85 ppm) and Nb (1 – 2 ppm) indicating that their magma was derived from a source mantle that experienced a previous melt extraction event. This is mainly because partial melting and melt extraction leaves a residual mantle depleted in the HFSE, a hypothesis that is commonly observed insubduction-related magmas (Pearce and Peate, 20). This mantle source is supposed to be located in the convecting ashtenosphere mantle wedge above the subducting slab (Davis and Stevenson, 21). The relative enrichment of LILE and LREE compared with HFSE has been also interpreted by many workers as the result of metasomatism of the mantle wedge by hydrous fluids driven off the subducted oceanic slab (e.g. McCulloch and Gamble, 22). The depletion of mantle peridotites as a result of partial melting followed later by enrichment in LILE and LREE has been proved in studies of peridotite nodules in basalts and alpine ultramafics

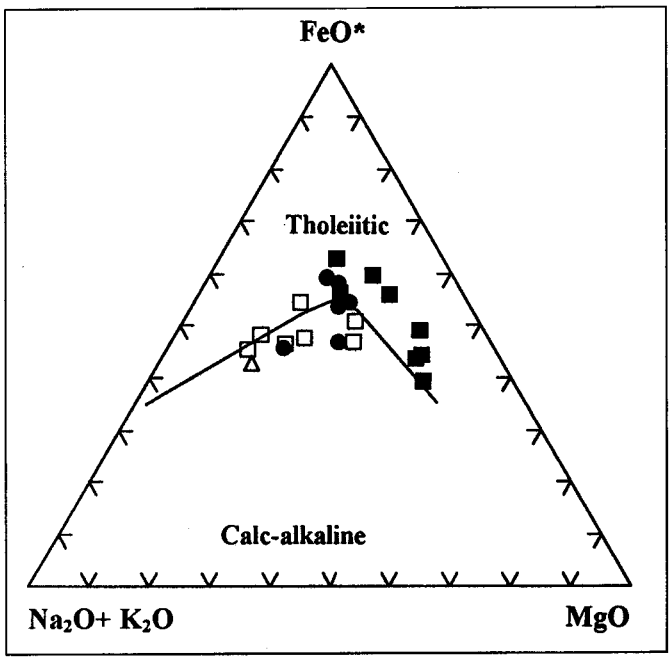

Fig. 5 : The AFM ternary plot for the Magal Gebriel volcanic rocks, (after Irvine and Bargar, 13). Symbols as in Fig. 2.

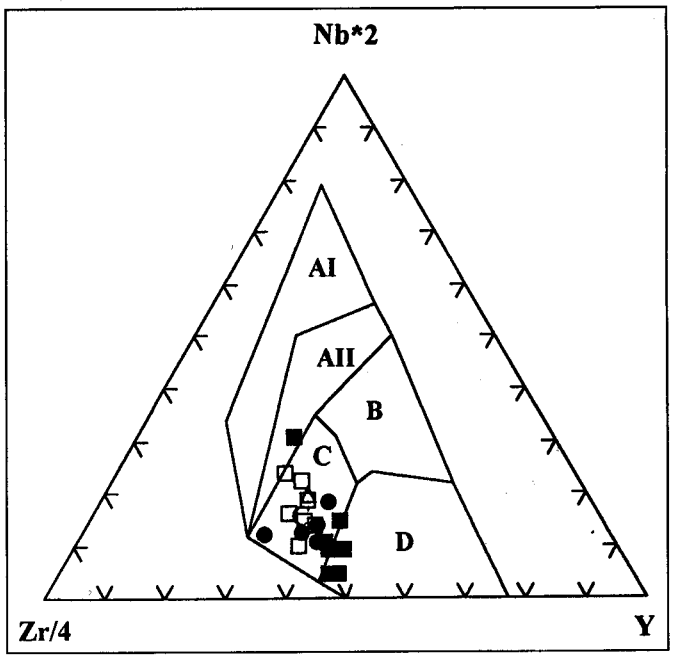

Fig. 6 : The Nb-Zr-Y discrimination diagram (after Meschede, 14) for the MGM. AI: within-plate alkali basalts, AII: within-plate alkali basalts and within-plate tholeiites, B: E-type MORB, C: within-plate tholeiites and volcanic-arc basalts, D: N-type MORB and volcanic-arc basalts. Symbols as in Fig. 2.

(Frey and Prinz, 23; Frey et al., 24). This has also been demonstrated by the metasomatized mantle xenoliths from suprasubduction zone regions (Maury et al., 25). The mantle wedge is considered to be the major locus of magma generation in subduction zones but there is a controversial question as to whether it has MORB-like characteristics (e.g. Perfit et al., 26) or oceanic island basalt characteristics (e.g. Saunders et al., 27). This leads to difficulties in assessing the sources and processes responsible for the genesis of island arc basalts.

Constraints on the composition and characteristics of the mantle source and extent of partial melting:

The REE patterns of oceanic island arcs are similar at geographically diverse locations suggesting that the sources and the processes of producing their magmas are not at random (Arth, 19). A uniformity of both source mineralogy and the process by which "least fractionated" magmas are generated may be implied. The chondrite-normalized REE patterns of the studied metavolcanic rocks have nearly flat HREE patterns $\{(Gd/Yb)_N = 1.2 - 1.5\}$ suggesting that they originated from a garnet-free peridotite source. The mother magma may represent partial melts of shallow (< 75 km) spinel-bearing mantle (cf. Menzies and Chazot, 28). Melting of this mantle source would produce the most primitive basaltic magmas in magal Gebriel area. Successive fractional crystallization of these primitive magmas yielded the voluminous tholeiitic/calc-alkaline varieties of Magal Gebriel volcanics.

In order to put constraints on the composition of mantle source region in which the parental magma of the MGM was generated, it is useful to compare the compositional data of the most primitive rocks with partial melting models of different endmember mantle reservoirs (Fig. 10). Non-model

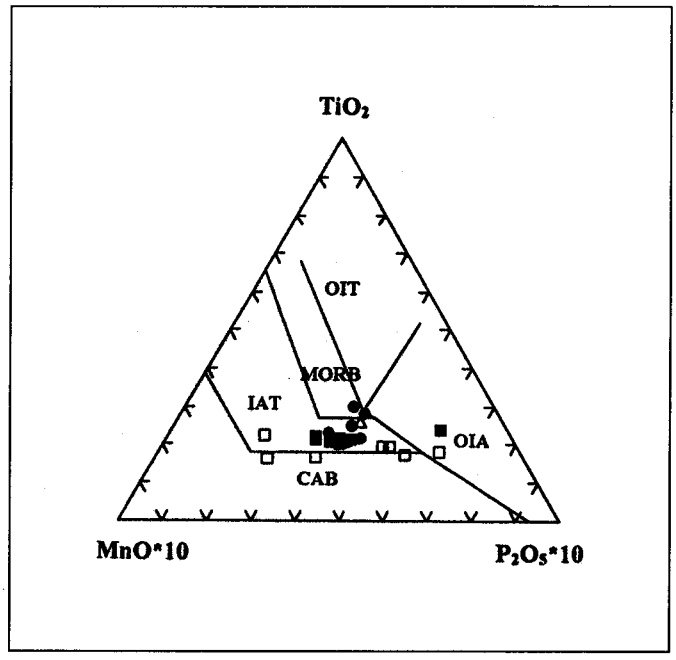

Fig. 7 : The TiO_2-MnO-P_2O_5 discrimination diagram (after Mullen, 15) for the MGM. OIT: ocean-sland tholeiite or semount tholeiite, MORB: mid-oceanic ridge basalt, IAT: island-arc tholeiite, CAB: island-arc calc-alkaline basalt, OIA: ocean-island alkali basalt or seamount alkali basalt. Symbols as in Fig. 2.

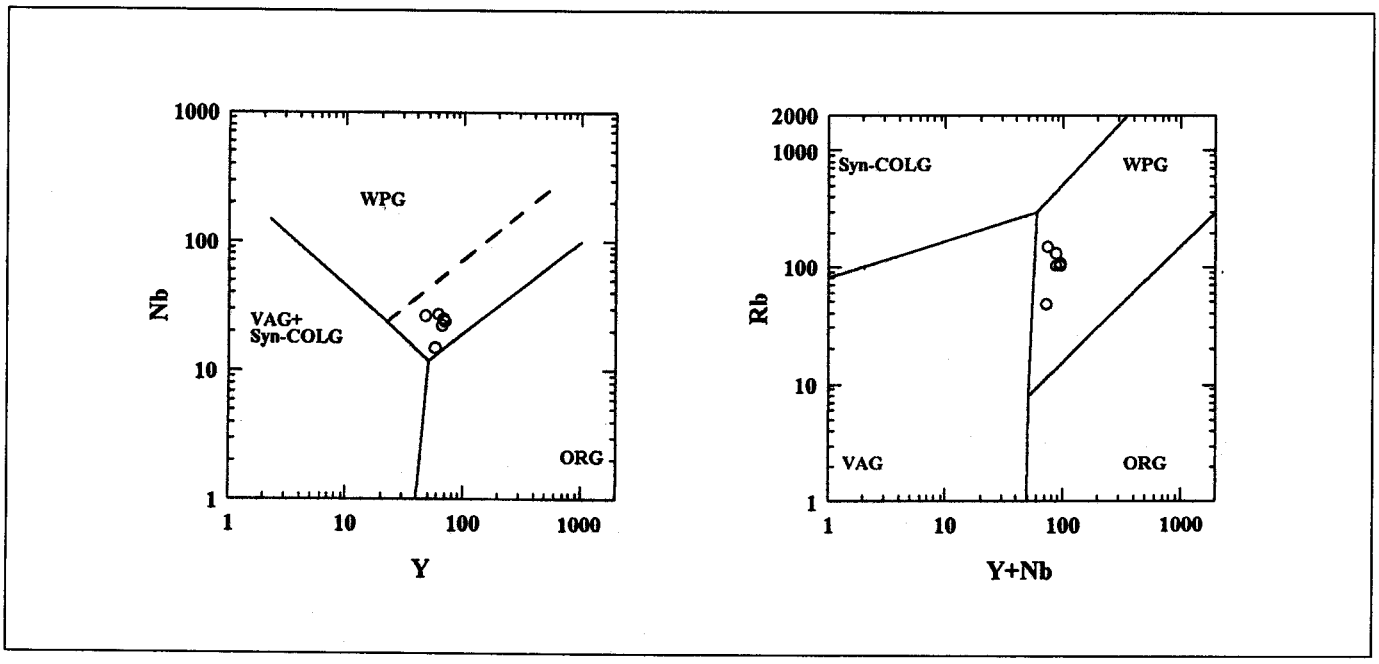

Fig. 8A & B : Discrimination diagrams of (A) Nb vs Y and (B) Rb vs (Y+Nb) for the Magal Gebriel rhyolitic rocks. WPG: within-plate granitoids, VAG: volcanic-arc granitoids, sys-COLG: syn-collision granitoids, ORG: ocean-ridge granitoids, (after Pearce et at., 16). Symbols as in Fig. 2.

total equilibrium melting was assumed in which the melt is continually reacting and reequilibrating with the residual melt until they are seperated. The equation of Shaw [29] has been used in the calculations. Partial melting of garnet-lherzolite produces REE patterns of lower HREE and higher LREE than the REE patterns of the most primitive varieties in MGM (Fig.11A). Similarly, the calculations show that partial melting of a garnet-bearing primitive mantle yields lower HREE patterns when the degree of melting ranges from 5 to 20% (Fig. 11B). The spinel-bearing primitive mantle source provides flat to gently dipping REE patterns, which are clearly different from the patterns of the most primitive varieties in MGM (Fig. 11D). In contrast, moderate degree of partial melting (15-20%) of aspinel-iherzolite source yields REE patterns that thave HREE abundances similar to the most primitive varieties in MGM in addition to lower LREE abundances (Fig. 11C). The latter model represents the best fit that can be obtained from the different mantle sources with regard to the distribution of HREE. However, this model yields very low abundances of LREE compared with those of the most primitive varieties in MGM, which cannot be interpreted only by the metasomatic effects and dehydration of the subducted slab that causes enrichment in the relatively mobile LREE.

Experimental data indicate that there is little or no enrichment of HFSE related to subduction processes, i.e. the HFSE are derived mainly from the mantle wedge (Stolper and Newman, 32; Brenan et al., 33; Pearce and Peate, 20). Thus, the internal consistency of HFSE ratios in the primitive rocks from MGM can be used to place constraints on the composition and extent of batch melting required to generate the primitive magma in Magal Gebriel area. Concentrations of Nb and Zr from the primitive rocks and some varieties of basaltic and andestic composition scatter about the values predicted for melting of a depleted mantle source and away from those predicted for melting of an enriched mantle source (Fig. 12). However, the abundances of Nb and Zr in the more differentiated rocks are greater than would be expected for direct melting of a mantle source. The estimated degrees of batch partial melting for the most primitive samples in MGM vary from 5 to 8% of the depleted mantle source (Fig. 12).

Compositional constraints of the subduction-derived component:

The enrichment of the subarc mantle for the MGM can be modeled using a procedure similar to that described by McCulloch and Gamble [22] in their study of Pacific rim island arc basalts. The concentration of an element in the depleted mantle wedge source region following enrichment by a slab-derived fluid component is given by the following mass balance equation:

$$C_{wi} = C_{dmi}\,(1\text{-}f_s) + C_{fluid\,(I)}\,(f_s) \qquad (1)$$

where Cwi is the concentration of element (I) in the wedge after it has been enriched, C_{dmi} is the concentration of element (I) in the depleted mantle wedge before the slab input, $C_{fluid\,(I)}$ is the concentration of element (I) in the slab-derived component, and fs is the fractional mass derived from the slab. We have calculated the mantle source composition (C_{wi}) for K_2O, Rb, Sr, Ba, La and Ce using the batch melting equation (Shaw, 29); the average extent of melting was derived from Zr and Nb data (Fig. 12). The values of the depleted mantle wedge (C_{dmi}) are obtained from Michael [34]. The absolute concentration of an element in the slab-derived component "$C_{fluid(i)}$" depends on the utilized model and f_s, and hence it is essentially arbitary, byt the ratios between the different elements are not (Stolper and Newman, 32). If the concentration of an element in the fluid is know or assumed, then the concnetrations of the other elements can be calculated using the following equation Michael, 34):

$$C_{fluid(i)}/C_{fluid(j)} = (C_{wi}\text{-}C_{dmi})/(C_{wj} - C_{dmj}) \qquad (2)$$

where (I) and (j) denote different elements and the other symbols are the same as defined in equation (1). We have assumed that the concentration of Ba in the slab-derived fluid component in is identical (1371 ppm, cf. Wallance and Carmichael, 35) to that calculated by Stolper and Newman [32] in their study of the subduction-related component in the Marianas.

The calculated concentrations of the different elements in the subduction-derived component (Table 2) are generally lower than those estimated for western Pacific island arcs (McCulloch and Gamble, 22; Stolper and Newman, 32) and for the subduction-derived component in Mexico (Wallace and Carmichael, 35). However, the estimated concentrations of K2O, Rb, Sr, Ba, La and Ce in the subduction-derived component relative to their concentrations in the depleted mantle (Table 2) are in the order Ba > Rb > K > La > Sr > Ce, similar to the order of enrichments deduced for arcs in the

Western Pacific (Pearce and Peate, 20) and in Maxico (Wallance and Carmichael, 35).

Generation of the rhyolitic rocks:

The rhyolites have nearly parallel REE patterns to those of the metavolcanic rocks. They posses also flat HREE patterns {$(Gd/Yb)_N$=1.01, on average} indicating that garnet is not involved in the source. These characteristics suggest similar parental magmas for both of the rhyolites and metavolcanic rocks, but the rhyolitic mother magma must have been subjected to severe differentiation and extraction of large amounts of plagioclase as indicated by the strong negative Eu anomalies (0.15, on average) and low Sr contrents (52 ppm, on average) exhibited by the rhyolites.

CONCLUSIONS

The volcanic suite in Magal Gebriel area comprises two contrasting units. The first one is metamorphosed in the

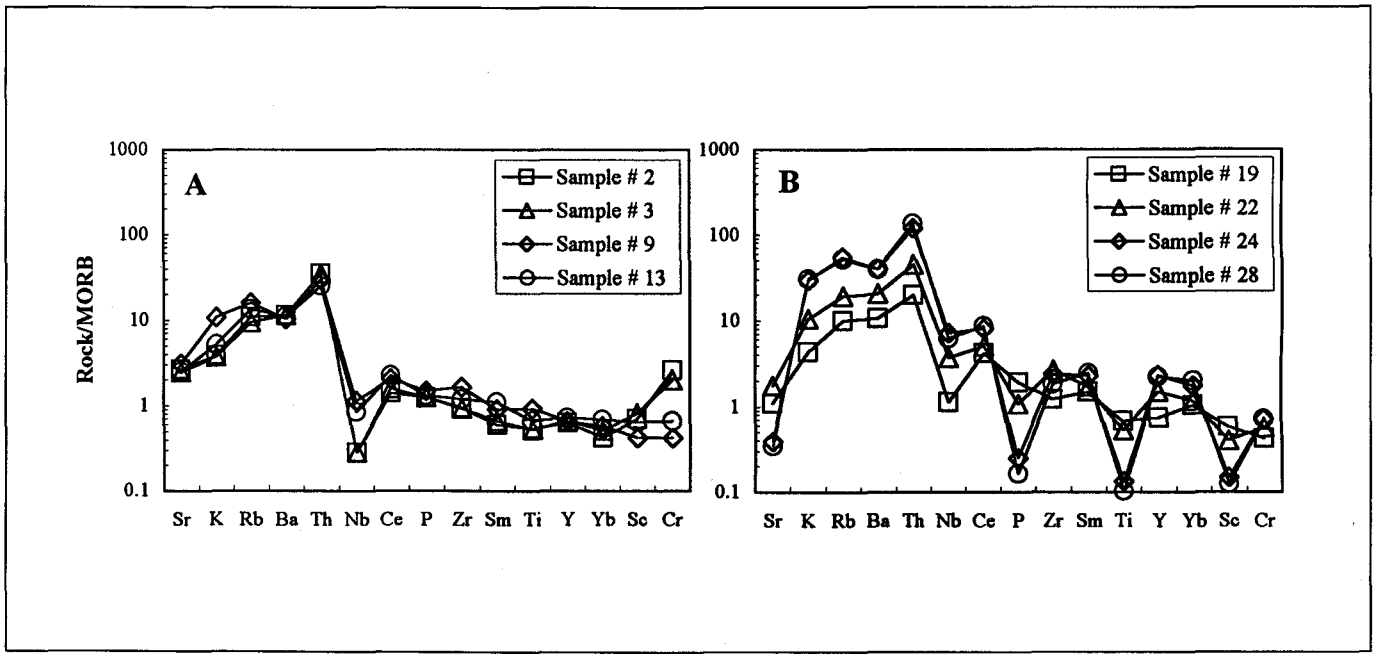

Fig. 9A & B: N-MORB-normalized patterns for the Magal Gebriel Volcanic rocks. Metabasalt: 2 and 3, Metabasaltic andestie: 9 and 13, Metandesite: 19, Metadacite: 22, Rhyolite: 24 and 28.

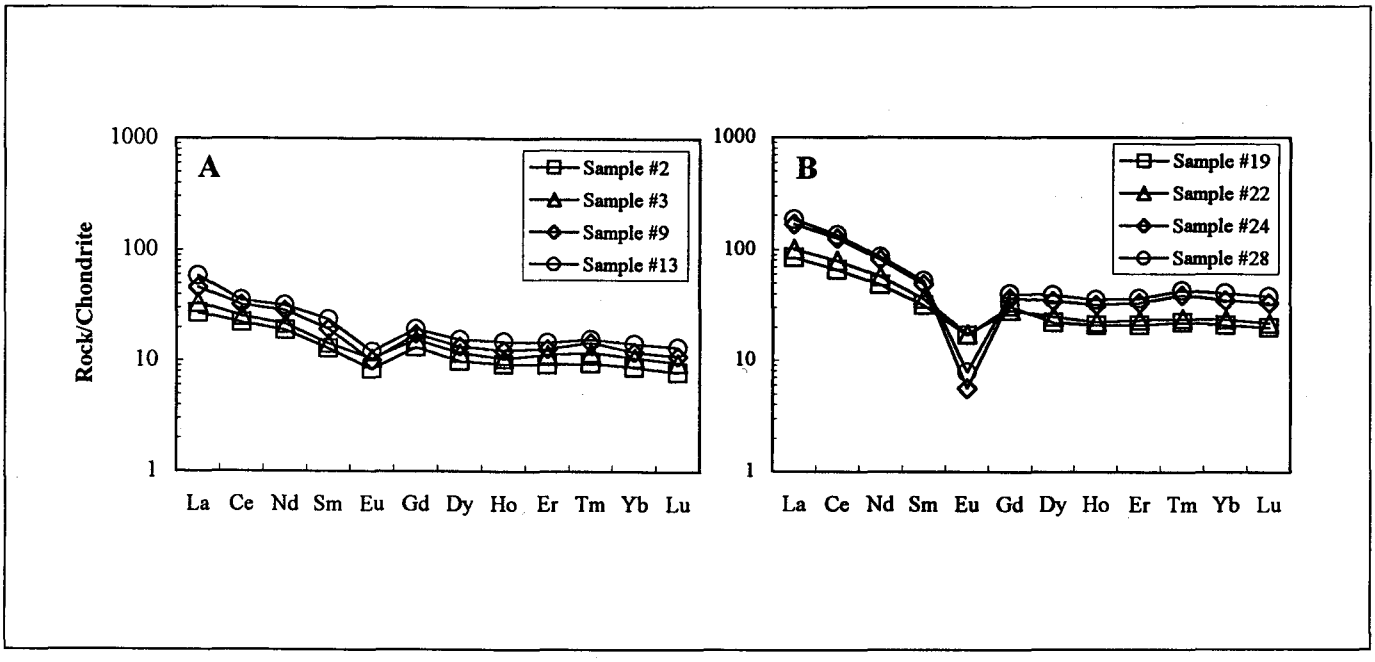

Fig. 10 A & B: Chondrite-normalized REE patterns for the Magal Gebriel volcanic rocks. Metabasalt: 2 and 3, Metabasaltic andesite: 9 and 13, Metandesite: 19, Metadacite: 22, Rhyolite: 24 and 28.

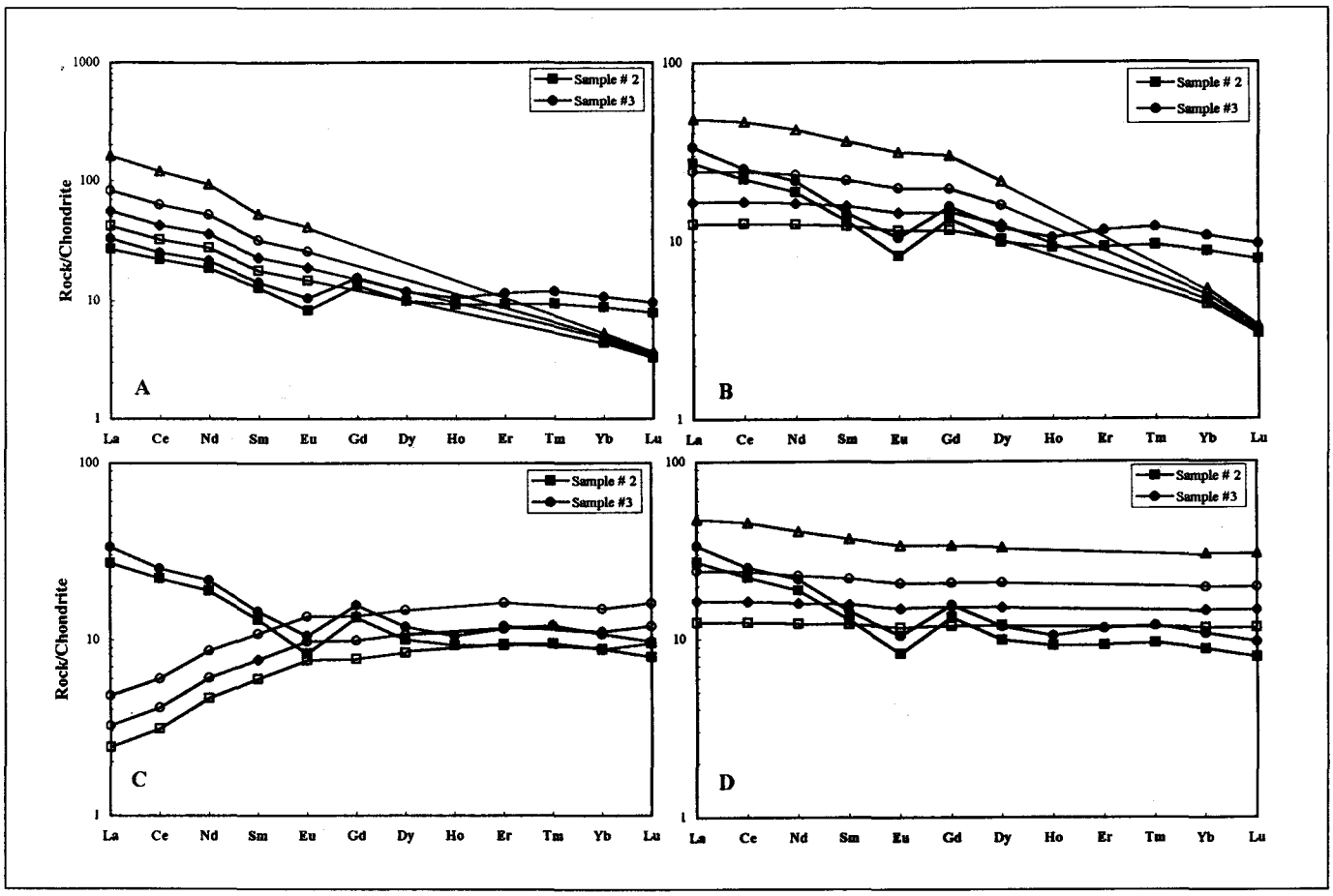

Fig. 11: Chondrite-normalized REE patterns of the most primitive varieties (Sample # 2 and 3) of MGM compared with calculated chondrite-normalized REE patterns for liquids resulting from 5 to 20% partial melting of several mantle sources with different REE values. A: Garnet-lherzolite (Bradshw et al., 30), B: Garnet-bearing primitive mantle (Hartmann and Wedephol, 31), C: Spinel-lherzolite (Hartmann and Wedephol, 31), D: Spinel-bearing primitive mantle: (Hartmann and Wedephol, 31). (Δ 5% partial melting, O :10% partial melting, ◇ : 15% partial melting, ❑: 20% partial melting.

greenschist to low amphibolite facies and ranges in composition from metabasalt to metadacite. This unit pertains to the younger metavolcanics. In contrast, the other unit is unmetamorphosed and has a rhyolitic composition with an age (654-665 Ma) slightly higher than that of the Dokhan Volcanics.

The metavolcanic rocks are subalkaline in nature with a transitional tholeiitic/calcaline affinity. They erupted in an island-arc tectonic setting and are characterized by enrichment in LILE and LREE and depletion in HFSE, suggesting that their parental magma were derived from a mantle source that has been depleted through a previous melt extraction event followed by enrichment in LILE and LREE via fluids from the subducted slab. The HREE of the metavolcanics have nearly flat patterns $\{(Gd/Yb)_N + 1.2 - 1.5\}$ indicating that they orginated from a garnet-free peridotite source. Model calculations show that the most primitive rocks from the Magal Gebriel metavolcanics (MGM) have been generated by low-degree partial melting (5-8%) of a depleted mantle source. Fractional crystallization is found to be an important process in the evolution of the mafic to the intermediate volcanic rocks at Magal Gebriel area by the removal of pyroxene, plagioclase and opaque minerals.

Model calculations have been used to put constraints on the composition of the subduction-derived component in Magal Gebriel area. These calculations show that the order of enrichment of the different mobile elements in the subduction-derived component is as follows: Ba > Rb > K > La > Sr > Ce, which is similar to the order deduced for arcs in the western Pacific and Mexico. However, the absolute values of these mobile elements are generally lower than those estimated in the island arcs of western Pacific and Mexico.

The rhyolitic rocks display a within-plate tectonic setting. They have parallel REE patterns to those of the metavolcanic rocks and exhibit also flat HREE patterns, suggesting similar

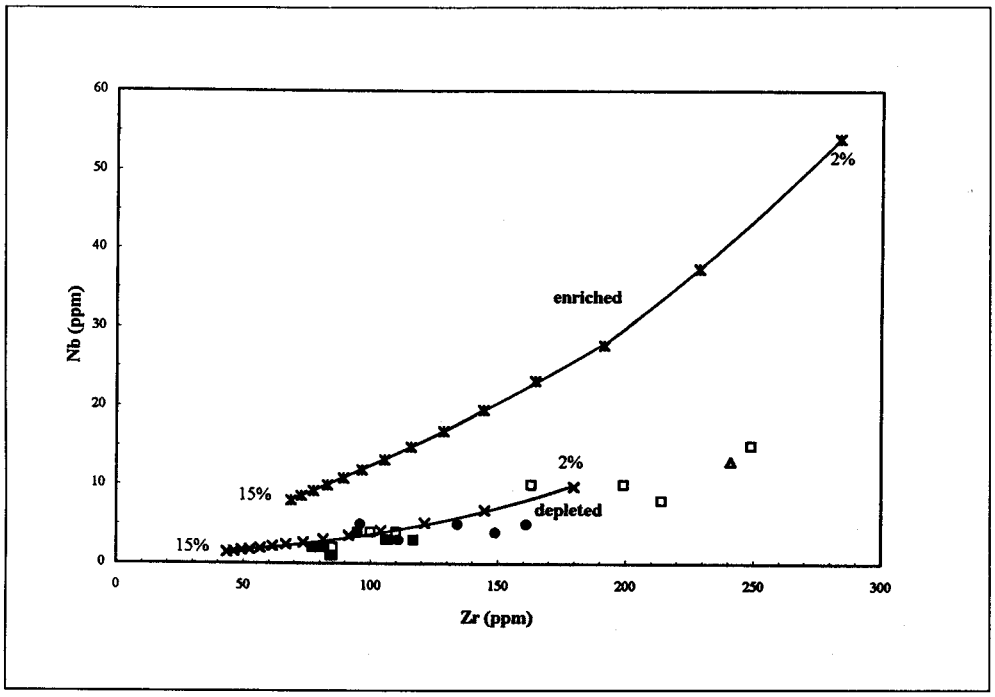

Fig. 12: Nb vs Zr diagram for the MGM. Curves show batch melting models for depleted and enriched mantle source regions calculated using compositional data from Michael [34]. Curves are marked in increments of 1% melting and show a maximum of 15% metling at far left.

parental magmas for the rhyolites and metavolcanic rocks. However, the strong negative Eu anomalies and low Sr contents of the rhyolitic rocks indicate that they were subjected to severe fractionation and extraction of large amounts of plagioclase.

ACKNOWLEDGEMENTS

We would like to thank with gratitude Prof. S. El-Gaby and Prof. S.O. Khali for reviewing and commenting on the manuscript. The analytical work was completed while the first author was a DAAD (German Academic Exchange Service) postdoctoral fellow at Germany. Many thanks to Prof. E. Seidel for providing facilities for major, trace and rare earth elements analyses.

REFERENCES

[1] **Stern, R.J. 1979.** Late Precambrian ensimatic volcanism in the Central Eastern Desert of Egypt, Ph.D. dissertation, 210p. University of California, San Diego, U.S.A.

[2] **Stern, R.J. 1981.** Petrogenesis and tectonic setting of late Precambrian ensimatic volcanic rocks, Central Eastern Desert, Egypt, Precambrian Res., 16: 195-230.

[3] **El-Gaby, S., Khudeir, A.A., Abdel Tawab, M. and Atalla, R.F. 1991.** The metamorphosed volcano-sedimentary succession at Wadi Kid, Southeastern Sinai Egypt, Annal. Geol. Surv., 17:19035.

[4] **Dixon, T.H. 1979.** Evolution of continental crust in the late Precambrian Egyptian Shield, Ph.D. dissertation, 231p. University of California, San Diego, U.S.A.

[5] **Stern, R.J. and Hedge, C.E. 1985.** Geochronologic and isotopic constraints on late Precambrian crustal evolution in the Eastern Desert of Egypy. Am. J. Sci., 285:97-127.

[6] **El-Gaby, S., List, F. K. and Tehrani, R. 1988.** Geology, evolution and metallogenesis of the Pan-African Belt in Egypt. In: El-Gaby, S. and Greilling R.D. (eds). The Pan African Belt of The North East Africa and Adjacent Areas, pp 17-68. Vieweg Verlag, Wiesbaden.

[7] **Farag, S.S. 1990.** Geology and radioactivity of Megal Gebriel area, Southeast Aswan, Egypt. Ms.Sc. dissertation, 141p. Al Azhar University, Egypt.

[8] **Hussein, H.A. Ali, M.M. and El-Ramly, M.F. 1982.** A proposed new classification of the granites of Egypt. J. Vol. Geoth. Res., 14: 187-198.

[9] **El-Shazly, E.M., Hashad, A. H., Sayyah, T.A., and Bassyuni, F.A. 1973.** Geochronology of Abu Swayel area, south Eastern Desert, Egypt.J. Geol., 17:1-18.

[10] **Winchester, J.A. and Floyd, P.A. 1977.** Geochemical discrimination of different magma series and their differentiation products using immobile elements. Chem. Geol., 20: 325-343.

[11] **Huges, G.J. 1973.** Spilites, Keratophyres and the igneous spectrum. Geol. Mag., 109: 513-527.

[12] **Davis, D.W., Blackburn, W.H., Brown, W.R. and Ehmann, W.D. 1978.** Trace element geochemistry and origin of late Precambrian-early Cambrian Catoctin greenstones of the Appalachian Mountains. University of California at Davies, unpublished report.

[13] **Irvine, T.N. and Baragar, W.R.A. 1971.** A guide to the classification of the common volcanic rocks. Can. J. Earth Sci., 8: 523-548.

[14] **Meschede, M. 1986.** A method of discriminating between different types of mid-ocean ridge basalts and continental tholeiites with the Nb-Zr-Y diagram. Chem. Geol., 56:207-218.

[15] **Mullen, E.D. 1983.** MnO/Tio2/P20o5: a minor element discriminant for basaltic rocks of oceanic environments and its implications for petrogenesis. Earth Planet. Sci. Lett., 62: 53-62.

[16] **Pearce, J.A., Harris, N.B.W. and Tindle, A.G. 1984.** Trace element discrimination diagrams for the tectonic interpretation of granitic rocks. J. Petrol., 25: 956-983.

[17] **Pearce, J.A. 1983.** Role of the sub-continental lithosphere in magma genesis at active continental margins. In: Hawkesworth, C.J. and Norry, M.J. (eds). Continental basalts and Mantle Xenoliths, pp 231-249. Shiva, Nantwich.

[18] **Saunders, A.D. and Tarney, J. 1979.** The geochemistry of basalts from a back-arc spreading center in the East Scotia Sea. Geochim. Cosmochim. Acta, 43:555-572.

[19] **Arth, J.S. 1981.** Rare-earth element geochemistry of the island-arc volcanic rocks of Rabaul and Talasea, new Britian. Geol. Soc. Am. Bull., 1-92:858-863.

[20] **Pearce, J.A. and Peate, D.W. 1995.** Tectonic implications of the composition of volcanic arc magmas. Ann. Rev. Earth Plante. Sci., 23: 251-285.

[21] **Davies, J.H. and Stevenson, D.J. 192\92.** Physical model of source region of subduction zone volcanics. J. Geophys. Res., 97: 2037-2070.

[22] **McCulloch, M.T. and Gamble, J.A. 1991.** Geochemical and geodynamical constraints on subduction zone magmatism. Earth Planet. Sci. Lett., 102: 358-374.

[23] **Frey, F.A. and Prinz, M. 1978.** Ultramafic inclusions from San Carlos, Arizona: petrologic and geochemical data bearing on their petrogenesis. Earth Planet. Sci. Lett., 38: 129-176.

[24] **Frey, F.A., Suen, C.J. and Stockman, H.W. 1985.** The Ronda high temperature peridotite. Geochemistry and petrogenesis. Geochim. Cosmochim. Acta, 49: 2469-2491.

[25] **Maury, R.C., Defant, M.J. and Joron, J-L. 1992.** Metasomatism of the sub-arc mantle inferred from trace elements in Philippine exenoliths. Nature, 360: 661-663.

[26] **Perfit, M.R., Gust, D.A., Bence, A.E., Arculus, R.J. and Taylor, S.R. 1980.** Chemical characteristics of island arc basalts: implications for mantle sources. Chem. Geol., 30:227-256.

[27] **Saunders, A.D., Norry, M.J. and Tarney, J. 1991.** Fluid infleunce on the trace element compositions of subduction zone magmas. Philos. Trans. Royal Soc., London, A, 335:337-392.

[28] **Menzies, M. and Chazot, G. 1995.** Fluid processes in diamond to spinel facies shallow mantle. J. Geodynam., 20:387-415.

[29] **Shaw, S.M. 1970.** Trace element fractionation during anatexis. Geochim. Cosmochim. Acta, 34:237-243.

[30] **Bradshaw, T.K., Hawkesworth, C.J. and Gallagher, K. 1993.** Basaltic volcanism in the Southern Basin and Range: no role for a mantle pulme. Earth Planet. Sci. Lett., 116:45-62.

[31] **Hartmann, G. and Wedepohl, K.H. 1993.** The composition of peridotite tectonites from the Ivrea Complex, northern Italy: residues from melt extraction. Geochim. Cosmochim. Acta, 57: 1761-1782.

[32] **Stolper, E.M. and Newman, S. 1994.** The role of water in the petrogenesis of Mariana trough magmas. Earth Planet. Sci. Lett: 121:293-325.

[33] **Brenan, J.M., Shaw, H.F., Ryerson, F.J. and Phinney, D.L. 1995.** Mineral aqueous fluid partitioning of trace elements chemistry of mantle and deep crustal fluids. Geochim. Cosmochim. Acta, 59:3331-3350.

[34] **Michael, P.J. 1988.** The concentration, behaviour and storage of H2o in the suboceanic upper mantle: implications for mantle metasomatism. Geochim. Cosmochim. Acta, 52:555-566.

[35] **Wallace, P.J. and Carmichael, I.S.E. 1999.** Quaternary volcanism near the Valley of Mexico: implications for subduction zone magmatism and the effects of crustal thickness variations on primitive magma compositions. Contrib. Mineral. Petrol., 135:291-314.

Table 1: Major, trace and REE abundances of the volcanic rocks of Magal Gebriel area.

Rock type	Metabasalt								Metabasaltic andesite						Metandesite							Metadacite	Rhyolite						
Sample #	1	2	3	4	5	6	7	8	9	10	11	12	13	14	15	16	17	18	19	20	21	22	23	24	25	26	27	28
SiO_2	47.84	48.73	48.94	49.14	49.21	50.06	50.50	51.35	52.64	53.59	53.62	54.05	54.34	54.75	55.75	55.94	57.39	57.76	58.67	61.49	62.66	65.15	72.02	74.83	75.61	75.71	76.30	76.59
TiO_2	3.63	0.82	0.79	1.22	0.84	0.81	0.98	0.95	1.41	1.48	1.13	0.86	1.01	0.98	0.60	1.27	0.82	0.50	1.04	0.95	0.90	0.80	0.40	0.20	0.12	0.19	0.08	0.14
Al_2O_3	13.73	15.85	15.49	16.40	15.62	15.21	15.65	15.54	15.93	18.60	14.73	17.57	17.67	15.08	17.43	16.92	16.11	14.23	12.01	16.06	15.13	14.19	13.00	12.57	12.71	12.51	12.80	12.06
Fe_2O_3*	15.60	8.78	9.62	12.80	9.51	10.33	10.59	11.32	9.98	9.53	12.00	9.01	8.88	10.24	8.96	9.52	8.98	7.34	10.37	7.53	7.31	6.24	4.99	1.52	1.07	1.44	0.84	1.22
MnO	0.23	0.15	0.15	0.21	0.17	0.17	0.20	0.19	0.15	0.16	0.18	0.12	0.18	0.18	0.15	0.13	0.23	0.18	0.16	0.14	0.14	0.10	0.10	0.03	0.05	0.02	0.09	0.02
MgO	4.39	9.15	8.45	4.81	8.31	7.62	5.46	4.67	5.31	3.63	3.62	3.74	3.81	3.51	4.54	3.54	3.71	4.27	3.04	2.03	1.96	2.04	0.59	0.24	0.18	0.23	0.09	0.14
CaO	7.52	9.91	10.36	7.72	10.52	10.92	10.69	10.70	7.09	3.06	7.10	8.76	9.21	8.68	6.24	2.79	4.59	10.03	6.06	4.50	5.01	4.13	2.44	0.77	0.52	0.74	0.40	0.45
Na_2O	2.88	2.37	2.18	3.17	1.89	1.53	1.94	2.09	3.18	3.55	3.13	2.72	2.07	2.53	2.97	4.08	4.93	2.09	4.07	3.41	3.39	3.88	4.06	3.68	4.09	3.72	4.20	3.65
K_2O	1.06	0.58	0.56	0.89	0.51	0.50	0.15	0.15	1.65	2.97	0.67	0.55	0.79	0.58	0.27	2.18	0.26	1.12	0.65	2.66	1.64	1.58	2.28	4.50	4.19	4.49	4.01	4.61
P_2O_5	0.93	0.15	0.15	0.24	0.13	0.13	0.18	0.19	0.18	0.22	0.23	0.14	0.16	0.20	0.06	0.45	0.18	0.08	0.34	0.25	0.23	0.13	0.06	0.03	0.02	0.03	b.d.	0.02
SO_3	0.19	0.03	0.02	0.04	0.02	0.03	0.04	0.04	0.10	0.03	0.03	0.08	0.04	0.05	0.04	b.d.	0.03	0.03	0.04	0.06	b.d.	0.04	b.d.	b.d.	0.03	b.d.	0.03	b.d.
L.O.I	1.41	2.66	2.49	2.64	2.59	2.65	2.88	2.80	2.15	2.46	2.76	2.54	2.10	2.99	2.56	2.62	2.49	2.17	2.67	0.76	0.87	1.20	0.91	0.86	0.82	0.77	0.69	0.40
Sum	99.41	99.18	99.20	99.28	99.32	99.96	99.26	99.99	99.77	99.26	99.21	100.14	100.26	99.77	99.57	99.44	99.72	99.80	99.12	99.84	99.24	99.48	100.85	99.23	99.41	99.85	99.53	99.30
Mg#	0.40	0.71	0.67	0.47	0.67	0.63	0.55	0.49	0.55	0.47	0.41	0.49	0.50	0.44	0.54	0.46	0.49	0.58	0.41	0.39	0.38	0.43	0.22	0.27	0.28	0.27	0.20	0.21
Sc	22	28	33	35	36	34	33	32	17	27	28	28	26	27	28	23	21	28	23	21	20	16	13	6	5	7	2	5
V	287	198	218	297	239	243	280	269	146	190	292	219	221	223	137	121	121	167	214	75	76	56	b.d.	10	6	8	b.d.	8
Cr	102	655	502	87	415	380	110	173	107	85	81	129	166	167	153	61	134	165	105	144	130	141	93	179	180	166	186	179
Co	35	38	34	34	38	36	39	33	38	30	34	27	22	25	29	19	28	21	20	16	15	18	4	b.d.	3	2	2	2
Ni	58	286	220	43	166	147	66	88	78	32	40	53	71	75	52	19	40	70	63	55	53	65	42	58	49	52	53	51
Cu	57	56	59	117	68	70	128	120	28	68	117	141	71	97	79	50	44	43	90	16	15	23	15	12	8	8	3	b.d.
Zn	147	64	68	101	67	69	91	82	137	117	88	59	98	90	91	92	90	59	66	76	77	75	19	38	61	39	66	51
Ga	22	12	14	19	13	14	18	19	19	19	16	17	16	18	19	19	16	11	9	16	18	16	17	17	21	18	22	17
Rb	23	22	19	13	18	18	4	7	32	92	6	20	27	15	7	60	8	23	20	69	45	39	48	109	132	103	149	104
Sr	502	318	298	325	281	263	447	449	372	130	316	295	301	525	277	185	284	184	133	150	153	212	119	47	31	41	29	42
Y	53	19	20	26	18	19	23	23	20	29	24	21	22	27	16	43	24	15	22	39	37	44	58	69	61	70	48	66
Zr	347	85	84	117	81	77	95	106	149	161	111	96	108	134	100	249	163	85	110	214	199	241	309	215	181	210	118	164
Nb	31	1	1	3	2	2	4	3	4	5	3	5	3	5	4	15	10	2	4	8	10	13	15	25	27	24	26	22
Cs	13	13	14	1	16	17	5	4	b.d.	25	6	6	16	8	20	11	b.d.	6	18	b.d.	20	5	5	2	2	3	b.d.	b.d.
Ba	367	230	228	458	223	220	57	98	207	507	122	117	223	334	198	995	267	198	213	1041	526	413	684	809	620	808	27	801
La		*6.65*	*8.21*						*11.34*				*14.32*						*20.74*			*24.60*		*41.60*				*45.31*
Ce		*14.20*	*16.15*						*20.70*				*22.72*						*42.29*			*51.00*		*80.81*				*86.34*
Nd		*8.92*	*10.30*						*13.50*				*15.15*						*22.97*			*27.30*		*38.90*				*40.51*
Sm		*1.98*	*2.20*						*3.01*				*3.64*						*4.90*			*5.61*		*7.56*				*8.07*
Eu		*0.48*	*0.61*						*0.58*				*0.70*						*0.99*			*1.02*		*0.33*				*0.46*
Gd		*2.71*	*3.17*						*3.57*				*3.99*						*6.31*			*5.87*		*7.50*				*8.23*
Dy		*2.51*	*2.98*						*3.42*				*3.95*						*5.66*			*6.34*		*8.93*				*10.04*
Ho		*0.52*	*0.59*						*0.70*				*0.85*						*1.20*			*1.28*		*1.83*				*2.04*
Er		*1.53*	*1.90*						*2.14*				*2.44*						*3.51*			*3.89*		*5.57*				*6.12*
Tm		*0.24*	*0.30*						*0.37*				*0.40*						*0.57*			*0.61*		*1.01*				*1.10*
Yb		*1.44*	*1.76*						*1.99*				*2.37*						*3.51*			*3.91*		*5.87*				*6.72*
Lu		*0.20*	*0.24*						*0.28*				*0.34*						*0.51*			*0.56*		*0.85*				*0.98*
W	b.d.	29	28	b.d.	26	25	7	9	11	b.d.	14	22	13	16	2	2	21	b.d.	14	7	7	10	16	15	28	12	31	13
Pb	7	5	6	5	6	5	6	5	12	1	1	6	11	5	3	4	4	1	2	13	9	6	10	19	20	20	23	26
Th	5	7	7	3	5	6	2	3	6	7	2	8	5	3	5	7	6	7	4	10	10	9	15	24	31	26	34	27
U	4	5	5	1	7	7	b.d.	2	2	5	b.d.	b.d.	3	3	3	b.d.	b.d.	2	3	5	3	3	4	2	6	3	8	3

Fe_2O_3 *= total iron as Fe_2O_3, b.d. = below detection limit

Table 2 : Composition of the subduction-related component in the Magal Gebriel area correlated with other areas.

	$C_{fluid(i)}$ (MGM)	MG 91	SN 94	WC 99
K_2O (wt%)	3.1	5.4	8.5	3.8
Rb (ppm)	121	124	147	72
Sr (ppm)	1336	4654	4681	2473
Ba (ppm)	1371	1371	1371	1371
La (ppm)	30	—	99	53
Ce (ppm)	47	27	—	91

MG 91: Subduction-related enriching component estimated by McCulloch and Gamble (1991) for Pacific Rim arc basalts.

SN 94: Subduction-related enriching component estimated by Stolper and Newman (1994) for Mariana Trough basalts (Western Pacific).

WC 99: Subduction-related enriching component estimated by Wallace and Carmichael (1999) for the Mexican Volcanic Belt.

All compositions are normalized to Ba= 1371 to facilitate comparison.